

# SATB2 suppresses the progression of colorectal cancer cells via inactivation of MEK5/ERK5 signaling

Mohammed A. Mansour<sup>1,2</sup>, Toshinori Hyodo<sup>1</sup>, Satoko Ito<sup>1</sup>, Kenji Kurita<sup>3</sup>, Toshio Kokuryo<sup>3</sup>, Keisuke Uehara<sup>3</sup>, Masato Nagino<sup>3</sup>, Masahide Takahashi<sup>4</sup>, Michinari Hamaguchi<sup>1</sup> and Takeshi Senga<sup>1</sup>

<sup>1</sup> Division of Cancer Biology, Nagoya University Graduate School of Medicine, Nagoya, Japan

<sup>2</sup> Biochemistry Section, Department of Chemistry, Faculty of Science, Tanta University, Egypt

<sup>3</sup> Department of Surgical Oncology, Nagoya University Graduate School of Medicine, Nagoya, Japan

<sup>4</sup> Department of Pathology, Nagoya University Graduate School of Medicine, Nagoya, Japan

## Keywords

colorectal cancer; ERK5; invasion; migration; SATB2

## Correspondence

T. Senga and M. A. Mansour, Division of Cancer Biology, Nagoya University Graduate School of Medicine, 65 Tsurumai, Showa, Nagoya 466-8550, Japan  
Fax: +81 52 744 2464  
Tel: +81 52 744 2463  
E-mails: tsenga@med.nagoya-u.ac.jp; biomansour@hotmail.com

(Received 18 November 2014, revised 15 January 2015, accepted 4 February 2015)

doi:10.1111/febs.13227

Special AT-rich sequence binding protein 2 (SATB2) is an evolutionarily conserved transcription factor that has multiple roles in neuronal development, osteoblast differentiation, and craniofacial patterning. SATB2 binds to the nuclear matrix attachment region, and regulates the expression of diverse sets of genes by altering chromatin structure. Recent studies have reported that high expression of SATB2 is associated with favorable prognosis in colorectal and laryngeal cancer; however, it remains uncertain whether SATB2 has tumor-suppressive functions in cancer cells. In this study, we examined the effects of SATB2 expression on the malignant characteristics of colorectal cancer cells. Expression of SATB2 repressed the proliferation of cancer cells *in vitro* and *in vivo*, and also suppressed their migration and invasion. Extracellular signal-regulated kinase 5 (ERK5) is a mitogen-activated protein kinase that is associated with an aggressive phenotype in various types of cancer. SATB2 expression reduced the activity of ERK5, and constitutive activation of ERK5 restored the proliferation, anchorage-independent growth, migration and invasion of SATB2-expressing cells. Our results demonstrate the existence of a novel regulatory mechanism of SATB2-mediated tumor suppression via ERK5 inactivation.

## Introduction

Colorectal cancer is the third most common cancer diagnosed in both men and women worldwide. More than 1 million new cases are clinically diagnosed each year, and more than 500 000 patients die from colorectal cancer annually [1]. As most colorectal cancer deaths are associated with tumor invasion and metastasis, there is a strong impetus to understand the function of cancer genes involved in colorectal cancer progression and invasiveness in order to develop new therapeutic approaches.

Special AT-rich sequence-binding protein 2 (SATB2) is a transcription factor that specifically binds to the nuclear matrix attachment region of DNA to regulate chromatin remodeling and transcription [2,3]. SATB2 comprises two CUT domains, which mediate associations with the matrix attachment region, and a homeobox domain at the C-terminus. When SATB2 is localized to the matrix attachment region, it promotes chromatin rearrangement by recruiting the nucleosome remodeling and histone deacetylase complex [4]. Stud-

## Abbreviations

AKT, v-akt murine thymoma viral oncogene homolog; ERK, extracellular signal-regulated kinase; MEK, mitogen-activated protein kinase kinase; SATB2, special AT-rich sequence binding protein 2.

ies have revealed that SATB2 has multiple roles in craniofacial patterning, brain development, and osteoblast differentiation [5–8]. Targeted deletion of SATB2 in mice resulted in multiple craniofacial abnormalities, including truncation of the mandible, shortening of the nasal and maxillary bones, malformations of the hyoid bone, and a cleft palate [5]. In humans, the chromosomal deletions of 2q33.1 that cause SATB2 haploinsufficiency are associated with a cleft or high palate, facial dysmorphism, and intellectual disability [9–14]. In addition to the crucial role of SATB2 in developmental processes, SATB2 is abundantly expressed in pre-B cells, and regulates expression of the immunoglobulin mu gene by binding to matrix attachment region sequences flanking the enhancer region [15].

Recent studies have indicated that SATB2 is associated with cancer progression. Immunohistochemical analyses of laryngeal squamous cell carcinoma cells showed that lower expression of SATB2 was correlated with advanced clinical staging, histological grade and tumor recurrence, and exogenous expression of SATB2 in laryngeal squamous cell carcinoma cells suppressed tumorigenicity *in vitro* and *in vivo* [16]. In colorectal cancer, high SATB2 expression is associated with a favorable prognosis and sensitivity to chemotherapy and radiation [17,18]. The expression of microRNA-31 (miR-31) is correlated with an unfavorable prognosis in colorectal cancer patients, and miR-31 expression was found to promote an aggressive cancer cell phenotype [19]. SATB2 is a direct target of miR-31, and expression of SATB2 attenuated the tumorigenicity induced by miR-31 [19]. These studies indicate a possible role for SATB2 as a tumor suppressor gene; however, a detailed analysis of SATB2 function in cancer cells has not been performed. In this study, we examine the effect of SATB2 expression in colorectal cancer cells. We show here that exogenous expression of SATB2 represses the aggressive phenotype of colorectal cancer cells, and that this effect is partly mediated by inactivation of extracellular signal regulated kinase 5 (ERK5).

## Results

### SATB2 mRNA is reduced in colon cancer samples and SATB2 expression reduces cancer cell proliferation *in vitro* and *in vivo*

To investigate whether SATB2 has a suppressive function on colorectal cancer, we first examined SATB2 mRNA levels in human colorectal cancer tissues by quantitative RT-PCR. SATB2 mRNA levels were reduced in 21 human colorectal cancerous specimens, with 15 samples showing more than fivefold decreases

in SATB2 mRNA compared with normal controls (Fig. 1A). We next examined the effects of exogenous expression of SATB2 on colorectal cancer cells. We established HCT116 and DLD-1 cells that constitutively expressed GFP or GFP-SATB2 by retrovirus infection. The level of exogenously expressed GFP-SATB2 was significantly higher than that of endogenous SATB2 (Fig. 1B). SATB2 expression induced the disruption of cell–cell adhesions, and the HCT116 cells became more spindle-shaped (Fig. 1C). Although the morphological changes were similar to those of the epithelial to mesenchymal transition, the expression of marker proteins such as E-cadherin, N-cadherin and vimentin was not affected (Fig. 1D). To determine whether SATB2 expression had any effect on cell growth, we performed a cell proliferation assay. As shown in Fig. 1E, SATB2 had a suppressive function on the proliferation of both HCT116 and DLD-1 cells.

Anchorage-independent growth is one of the critical aspects of tumor cells. To explore whether SATB2 expression inhibits the anchorage-independent growth of colorectal cancer cells, SATB2-expressing cells were cultured in soft agar. Two weeks later, the number of colonies and mean colony size were determined. The results showed clear suppression of the growth of SATB2-expressing cells in the absence of cell adhesion to the extracellular matrix (Fig. 2A). We next examined the proliferation of SATB2-expressing cells *in vivo*. Either GFP- or SATB2-expressing DLD-1 cells were subcutaneously injected into both sides of the femoral area of nude mice, and tumor formation was examined. As shown in Fig. 2B, tumor formation in response to injection of SATB2-expressing cells was suppressed compared with that in response to injection of GFP-expressing cells. The mice were killed 45 days after tumor cell injection, and the tumor weight was determined. The mean tumor weight in response to injection of SATB2-expressing cells was significantly reduced compared with that in response to injection of GFP-expressing cells (Fig. 2C). We also performed a 3D spheroid assay using HCT116 cells, which have a reduced ability to grow *in vivo*. SATB2 expression decreased the number and size of spheroids compared with GFP expression (Fig. 2D). These results show that SATB2 has a suppressive effect on cancer proliferation both *in vitro* and *in vivo*.

### SATB2 expression inhibits tumor migration and invasion

We next studied the effects of SATB2 expression on migration and invasion. To evaluate cell migration, we performed a wound-healing assay. Confluent

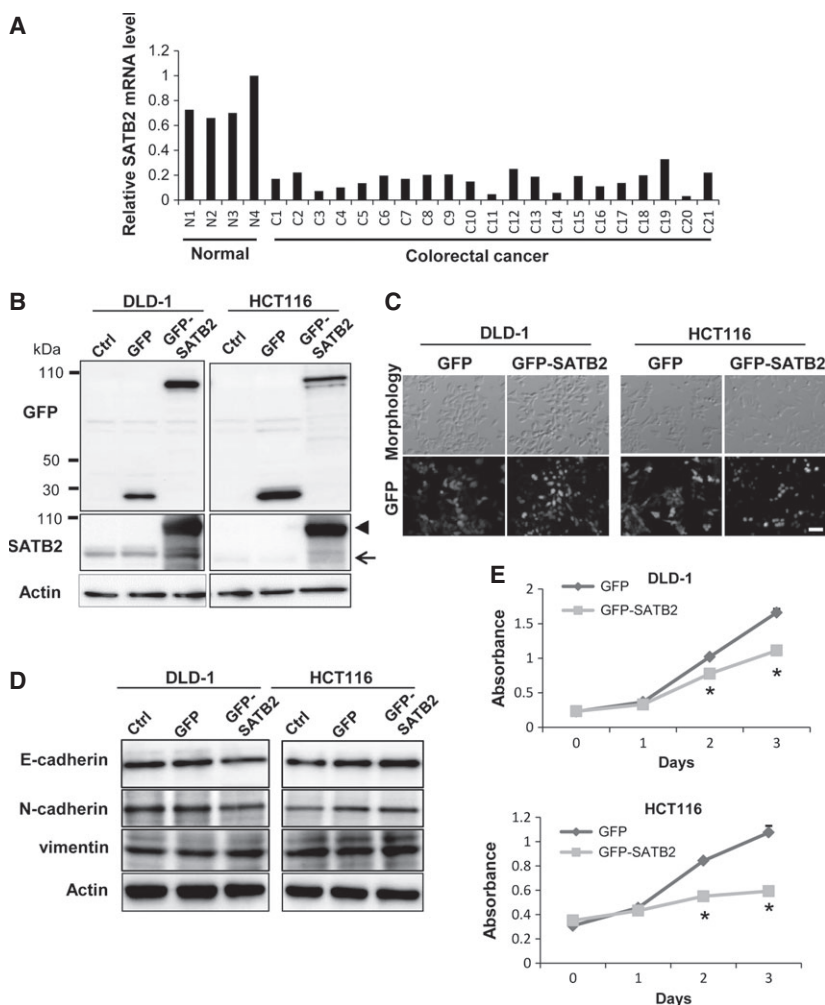


**Fig. 1.** SATB2 expression suppresses colorectal cancer cell proliferation. (A) The level of SATB2 mRNA in colorectal cancer specimens and normal colorectal tissues was evaluated by quantitative RT-PCR. The graph indicates relative SATB2 mRNA levels. (B) HCT116 and DLD-1 cells constitutively expressing GFP or GFP-tagged SATB2 (GFP-SATB2) were generated by retroviral infection. The expression of GFP or GFP-SATB2 proteins in each cell line was examined by immunoblotting. 'Ctrl' indicates parental HCT116 or DLD-1 cells. The arrow indicates endogenous SATB2 and the arrowhead indicates GFP-SATB2. (C) Representative images showing the cellular morphology of each cell line and GFP fluorescence. Scale bar = 50  $\mu$ m. (D) The expression of E-cadherin, N-cadherin and vimentin was examined by immunoblotting. (E) The number of viable cells at the indicated time points was determined using a Cell Counting Kit 8 (Dojindo).

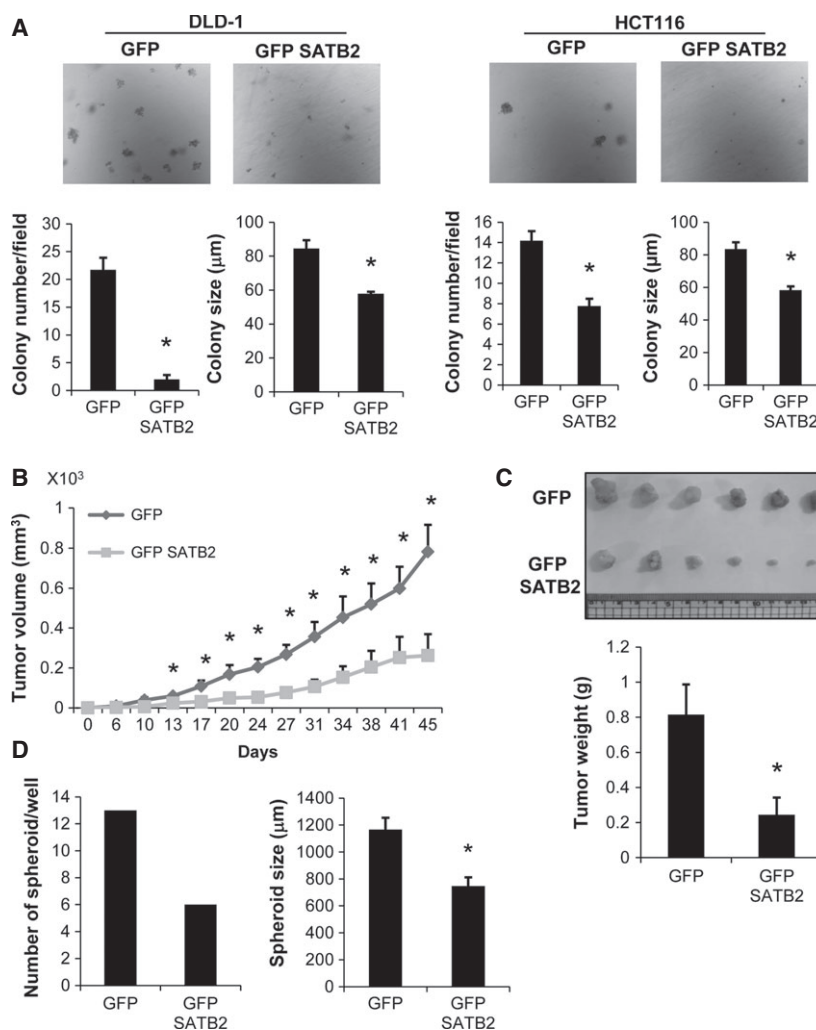
monolayers of GFP- or GFP-SATB2-expressing HCT116 cells were scratched, and the distance traveled by the migrating leading edges was measured every 12 h. We found a significant reduction in migration of SATB2-expressing HCT116 cells (Fig. 3A). To evaluate cell invasion, we used Matrigel-coated Boyden chambers: cells were seeded in the upper chamber, and cells invading the lower surface were counted 24 h later. As shown in Fig. 3B, a significant reduction in the number of invading cells was observed for SATB2 expression. Although reductions in both migration and invasion due to SATB2 expression were observed using HCT116 cells, SATB2 expression did not suppress migration and invasion in DLD-1 cells (data not shown).

### The CUT domain is essential for the suppressive function of SATB2

SATB2 has two independent characteristic domains: the homeobox domain and the CUT domains. The

CUT domain is a DNA-binding domain that is often found with a homeobox domain. There are two tandem CUT domains followed by one homeobox domain in SATB2. We created the deletion constructs shown in Fig. 4A, and investigated which regions are essential for the suppressive function of SATB2. A retrovirus encoding each GFP-tagged deletion was infected into HCT116 cells, and stable cell lines were established by puromycin selection. An immunoblot analysis confirmed the expression of each construct at the expected molecular weight (Fig. 4B). FL (full length),  $\Delta$ CUT and  $\Delta$ HOX accumulated in the nucleus, whereas  $\Delta$ N localized to both the nucleus and cytoplasm, indicating that the N-terminal portion is important for SATB2 accumulation in the nucleus (Fig. 4C). The expression of  $\Delta$ HOX induced morphological changes in HCT116 cells that were similar to those induced by expression of FL SATB2, but neither  $\Delta$ CUT nor  $\Delta$ N had any effect on the morphology of HCT116 cells (Fig. 4C). Cell proliferation and

**Fig. 2.** SATB2 suppresses anchorage-independent growth and *in vivo* tumor growth. (A) GFP- or GFP-SATB2-expressing cells were subjected to a colony formation assay. Representative images are shown, and the graphs indicate the mean number and size of colonies per field. (B) GFP- and GFP-SATB2-expressing DLD-1 cells were subcutaneously injected into the femurs of mice, and tumor volumes were measured. The graph shows the mean volume of six tumors corresponding to each cell line. (C) Forty-five days after tumor injection, the mice were killed, and tumor weights were measured. The images show the extracted tumors, and the graph indicates the mean tumor weight of the six tumors derived from each cell line. (D) GFP- or GFP-SATB2-expressing HCT116 cells were subjected to a spheroid formation assay. The graphs indicate the number of spheroids per well and the mean size of spheroids. Asterisks indicate values that are statistically significantly different from those of the control ( $P < 0.05$ ).



colony formation assays revealed that  $\Delta\text{HOX}$ , but not  $\Delta\text{CUT}$  or  $\Delta\text{N}$ , suppresses the proliferation and anchorage-independent growth of HCT116 cells (Fig. 4D,E). Consistent with these results, the migration and invasion of HCT116 cells were suppressed by  $\Delta\text{HOX}$  expression but not by  $\Delta\text{CUT}$  and  $\Delta\text{N}$  expression (Fig. 4F,G). These results indicate that both the N-terminal portion and the CUT domains are essential for the tumor-suppressive function of SATB2.

### Phosphorylation of ERK5 is reduced by SATB2 expression

After an extensive search for the molecular basis by which SATB2 expression suppresses the malignant characteristics of cancer cells, we found that phosphorylation of ERK5 was reduced by SATB2 expression in both HCT116 and DLD-1 cells. This reduction in

ERK5 phosphorylation was detected using either a phospho-specific antibody or ERK5 mobility shift (Fig. 5A). The phosphorylation of other signaling proteins, such as ERK1/2 and v-akt murine thymoma viral oncogene homolog (AKT), was not affected by SATB2 expression (Fig. 5A). To determine whether inactivation of ERK5 inhibits the malignant characteristics of cancer cells, we established HCT116 cells that constitutively expressed a dominant-negative form of MEK5 (DN-MEK5). As shown in Fig. 5B, expression of DN-MEK5 suppressed ERK5 phosphorylation but did not affect ERK1/2 phosphorylation. The expression of DN-MEK5 clearly suppressed the ability of HCT116 cells to grow in an anchorage-independent manner (Fig. 5C). In addition, both migration and invasion were inhibited by DN-MEK5 expression (Fig. 5D,E). These results demonstrate the critical role of ERK5 in the anchorage-independent growth, migration and invasion of HCT116 cells.

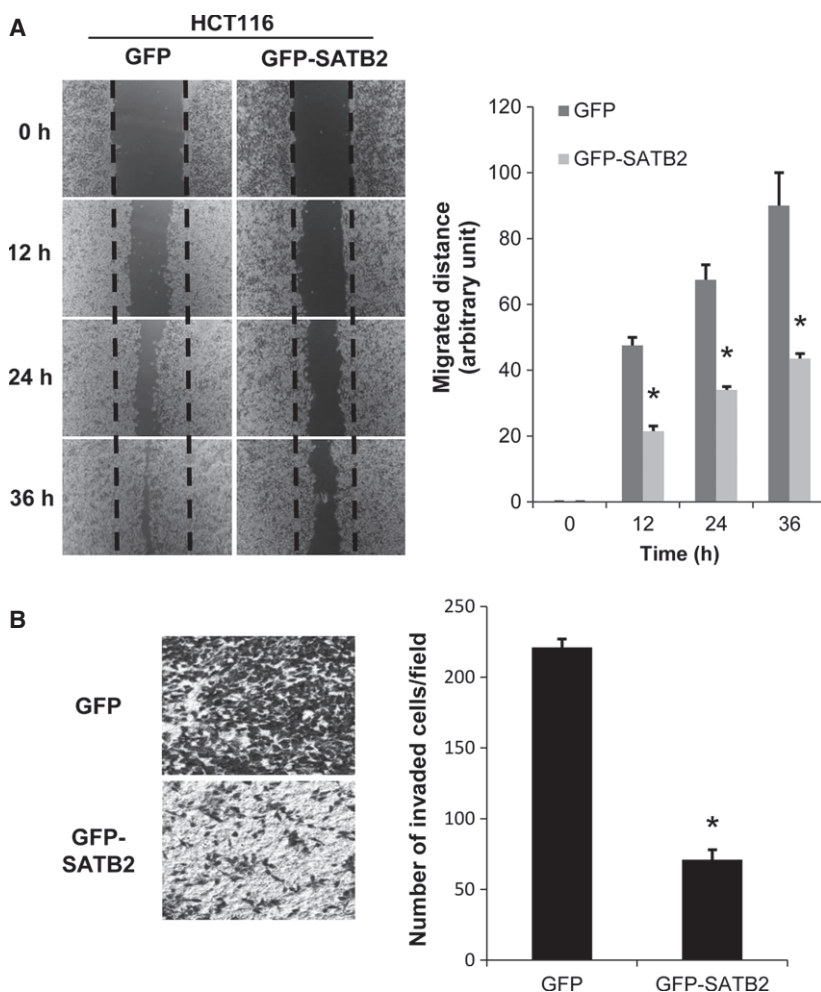


**Fig. 3.** SATB2 suppresses cancer cell migration and invasion. (A) Confluent monolayers of GFP- or GFP-SATB2-expressing HCT116 cells were scratched, and cell migration was examined every 12 h. Representative images of migrated cells are shown, and the graph shows the mean migrated distance at the indicated time points. (B) GFP- or GFP-SATB2-expressing HCT116 cells were subjected to an invasion assay. Representative images of invaded cells are shown, and the graph indicates the mean number of invaded cells per field. Asterisks indicate values that are statistically significantly different from those of the control ( $P < 0.05$ ).

### Activation of ERK5 restores the malignant characteristics of SATB2-expressing cells

We next investigated whether activation of ERK5 restored the malignant characteristics of SATB2-expressing cells. To activate ERK5, we used a constitutively active form of MEK5 (CA-MEK5). HCT116 cells that constitutively expressed SATB2 and FLAG-tagged CA-MEK5 (SATB2/CA-MEK5) or SATB2 and the FLAG tag (SATB2/FLAG) were generated by retrovirus infection. The active form of ERK5 was clearly increased in the SATB2/CA-MEK5-expressing HCT116 cells (Fig. 6A). We first examined the recovery of cell proliferation by ERK5 activation. As shown in Fig. 6B, the reduced cell growth due to SATB2 expression was partially restored by ERK5 activation. We also examined anchorage-independent growth, migration and invasion in SATB2/CA-MEK5 cells. ERK5 activation restored the ability of SATB2-expressing HCT116 cells to grow under anchorage-independent conditions (Fig. 6C). Similarly, ERK5

activation promoted the migration and invasion of SATB2-expressing HCT116 cells (Fig. 6D,E). Together, these results indicate that the tumor-suppressive function of SATB2 is partly mediated by inactivation of ERK5.

### Discussion

In this study, we examined the effects of SATB2 expression in various colorectal cancer cell lines. The proliferation and anchorage-independent growth of these cell lines were significantly repressed by SATB2 expression. Our tumor implantation experiment showed suppression of DLD-1 cell growth in mice by SATB2 expression. SATB2 expression reduced the migration and invasion of HCT116 cells, whereas knockdown of SATB2 in DLD-1 cells increased anchorage-independent growth and invasion. A previous study reported that SATB2 had inhibitory effects on the growth of laryngeal squamous cell carcinoma

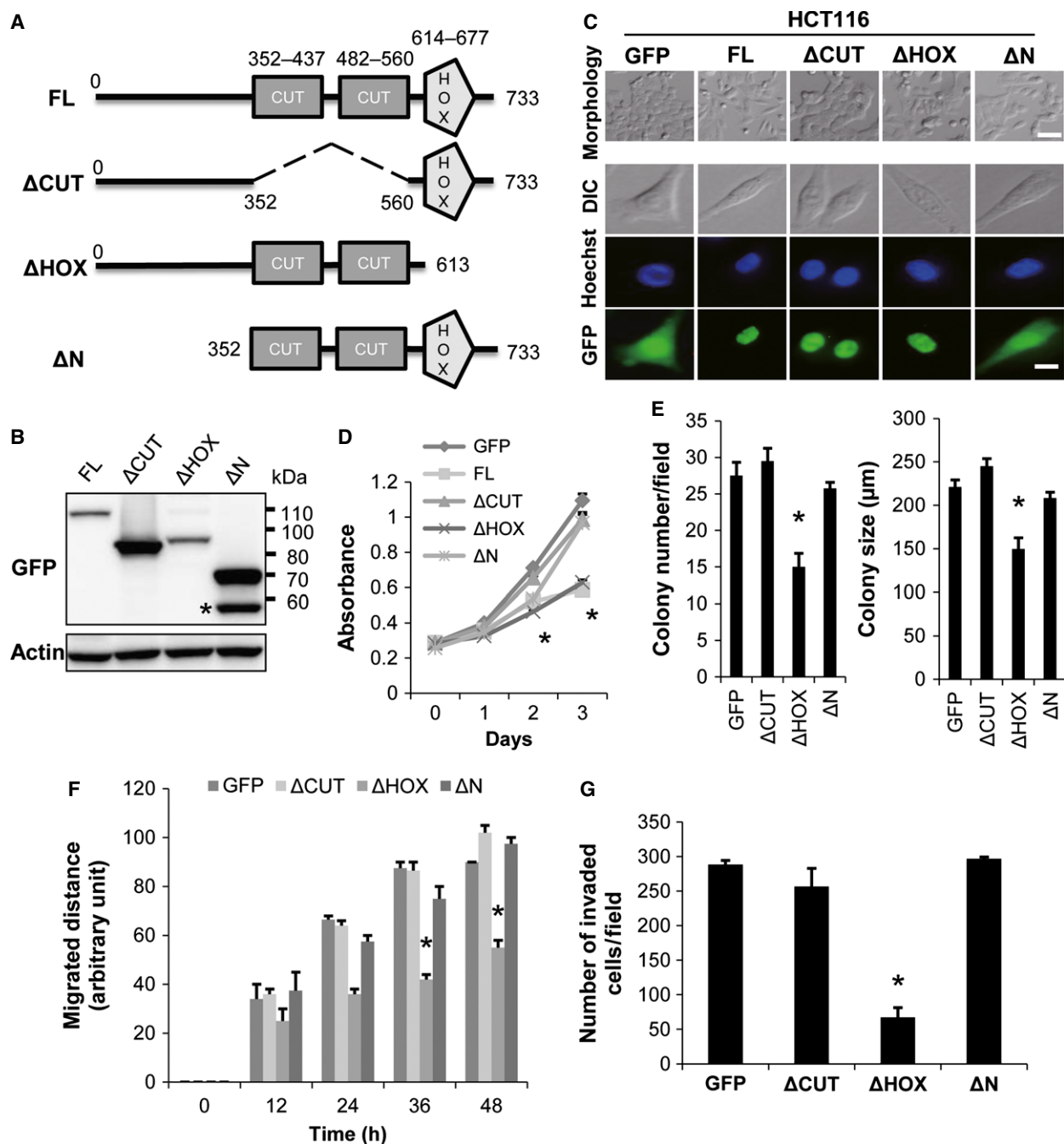


**Fig. 4.** The CUT domain is essential for the suppressive function of SATB2. (A) Structures of full-length SATB2 and deletion mutants. (B) HCT116 cells constitutively expressing each deletion mutant with a GFP tag were established by retrovirus infection. The expression of the indicated proteins in each cell line was examined by immunoblotting. The asterisk indicates a cleaved form of  $\Delta N$  SATB2. (C) Representative images of the cell morphology and fluorescence of HCT116 cells expressing each deletion mutant. Upper panel: morphology of mutant cells; scale bar = 50  $\mu\text{m}$ . Middle and bottom panels: localization of mutant SATB2; scale bar = 20  $\mu\text{m}$ . (D) The number of viable cells at the indicated time points was evaluated. (E) Each cell line was subjected to a colony formation assay. The graphs indicate the mean number and size of colonies per fields. (F) A wound healing assay was performed, and the mean migrated distance at the indicated time points is shown. (G) An invasion assay was performed, and representative images of invaded cells are shown. The graph indicates the mean number of invaded cells per field. Asterisks indicate values that are statistically significantly different from those of the control ( $P < 0.05$ ).

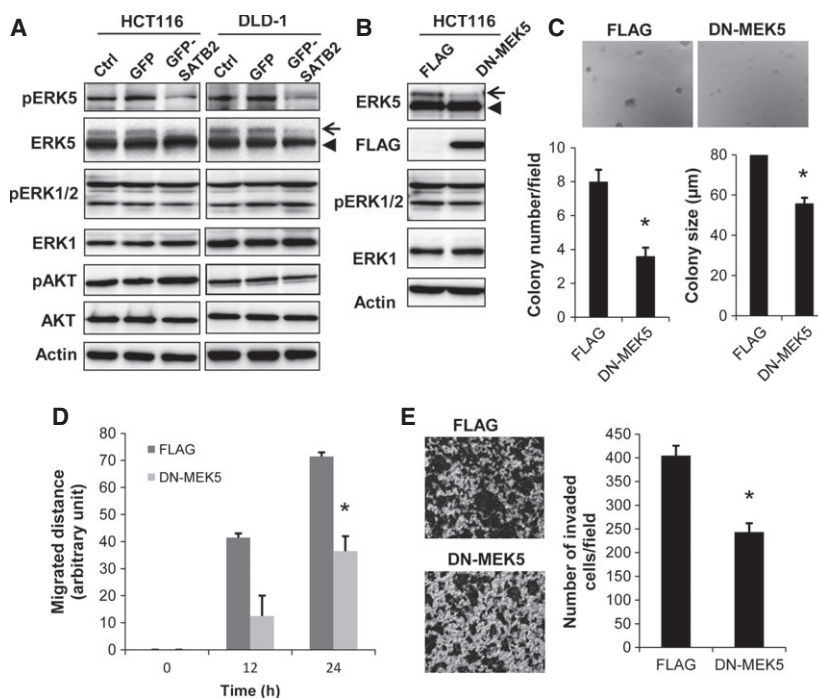


**Fig. 5.** SATB2 reduces the phosphorylation of ERK5, and inactivation of ERK5 suppresses colony formation, migration and invasion. (A) Immunoblot analysis of the phosphorylation and expression of the indicated proteins. The arrow indicates the mobility shift of the phosphorylated active form of ERK5, and the arrowhead indicates non-phosphorylated ERK5. (B) HCT116 cells constitutively expressing the FLAG tag or FLAG-tagged DN-MEK5 (dominant-negative MEK5) were generated by retrovirus infection. The phosphorylation and expression of the indicated proteins were examined by immunoblotting. The arrow indicates phosphorylated ERK5 and the arrowhead indicates non-phosphorylated ERK5. (C) FLAG- and DN-MEK5-expressing cells were subjected to a colony formation assay. Representative images are shown, and the graphs indicate the mean number and size of colonies per field. (D) A wound healing assay was performed, and the distance of the migrated cells was measured at the indicated time points. (E) An invasion assay was performed, and representative images of invaded cells are shown. The graph indicates the mean number of invaded cells per field. Asterisks indicate values that are statistically significantly different from those of the control ( $P < 0.05$ ).

cells in nude mice [16]. Together with this previous finding, our results clearly indicate that SATB2 suppresses the aggressive characteristics of cancer cells.

Our analysis using deletion constructs revealed that the N-terminal portion as well as the CUT domains were essential for the suppressive function of SATB2. It was rather surprising that deletion of the homeobox domain did not affect SATB2 function. The homeobox domain binds to conserved DNA sequences to promote transcription of target genes; therefore, deletion of this domain often disrupts the function of homeobox proteins [20]. It appears that homeobox domain-mediated transcriptional regulation is dispensable for the tumor-suppressive functions of SATB2, whereas binding to the AT-rich matrix attachment region sequences for chromosomal remodeling plays a critical role in SATB2 function. Interestingly, the N-terminal portion was also required for SATB2 function. The N-terminal region was found to be required for proper localization of SATB2 because deletion of the

N-terminus inhibited accumulation of the protein in the nucleus. Although the N-terminal region of SATB2 does not have any specific motifs, the region is highly conserved between SATB2 and its homolog SATB1. The N-terminal region of SATB1 has been reported to mediate dimerization of the protein [21]; therefore, dimerization of SATB2 may be required for proper localization to the nucleus and protein function.

ERK5 is a member of the mitogen-activated protein kinase family, and is activated in response to a plethora of extracellular stimuli, such as cytokines, growth factors, shear stress and hypoxia [22]. ERK5 is over-expressed in several carcinomas, and its role as a tumor-promoting factor has been well documented [23]. Immunohistochemical analysis demonstrated that phosphorylation of MEK5 was correlated with invasion, lymph node metastasis and staging of colorectal cancer [24]. The activation of ERK5 promotes the expression of matrix metalloproteinase 9, which is essential for degradation of the extracellular matrix for

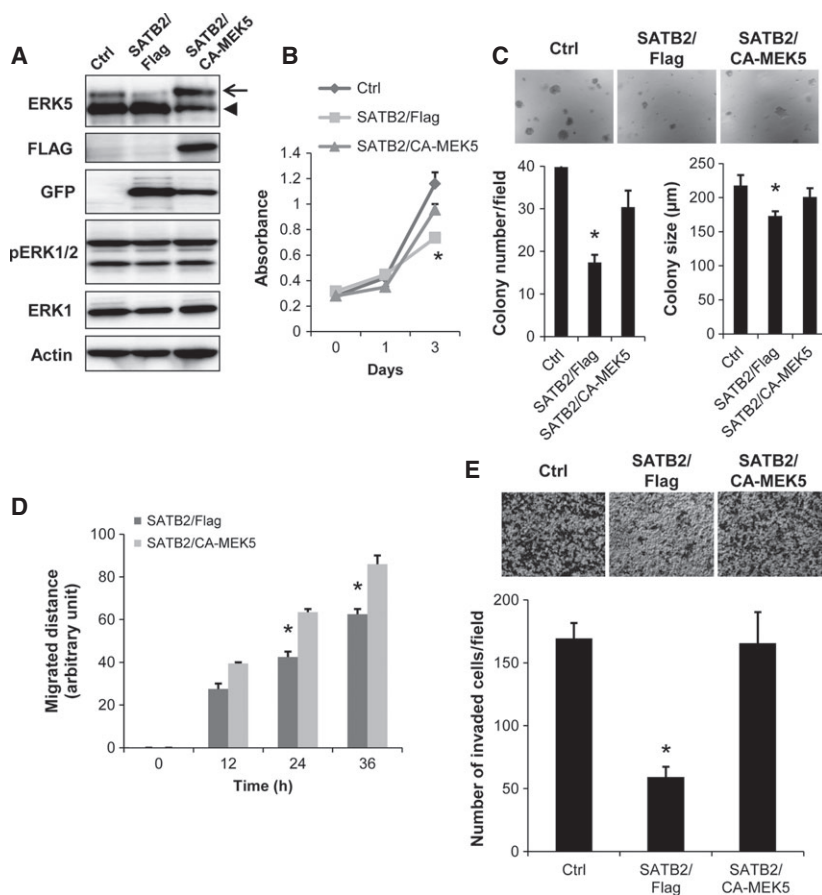


**Fig. 6.** ERK5 activation restores the malignant characteristics of SATB2-expressing cells. (A) HCT116 cells constitutively expressing SATB2 and the FLAG-tagged active form of MEK5 (SATB2/CA-MEK5) or SATB2 and the FLAG tag (SATB2/FLAG) were established by retrovirus infection. The phosphorylation and expression of the indicated proteins in both cell lines were examined by immunoblotting. 'Ctrl' indicates parental HCT116 cells. The arrow indicates the phosphorylated ERK5, and the arrowhead indicates non-phosphorylated ERK5. (B) The graph indicates the number of viable cells at the indicated time points. (C) SATB2/FLAG and SATB2/CA-MEK5 HCT116 cells were subjected to a colony formation assay. Representative images are shown, and the graphs indicate the mean number and size of colonies per field. (D) A wound-healing assay was performed, and the graph indicates the mean migrated distance of SATB2/FLAG and SATB2/CA-MEK5 HCT116 cells at the indicated time points. (E) An invasion assay was performed, and representative images of invaded cells are shown. The graph indicates the mean number of invaded cells per field. Asterisks indicate values that are statistically significantly different from those of the control ( $P < 0.05$ ).

invasion [25]. In addition, ERK5 induces actin cytoskeleton remodeling to promote cell migration and the formation of invadopodia, actin-based protrusions of the plasma membrane that are necessary for invasion [26]. We found that SATB2 expression reduced the phosphorylation of ERK5 in HCT116 and DLD-1 cells. The inactivation of ERK5 attenuated the malignant characteristics of HCT116 cells, and the activation of ERK5 recovered the ability of SATB2-expressing cells to migrate, invade and grow in soft agar. These results clearly indicate that inactivation of ERK5 is associated with the tumor inhibitory functions of SATB2. A previous study reported that expression of microRNAs related to mitogen-activated

protein kinase signaling was attenuated by SATB2 expression [27]; thus, the expression of proteins necessary for ERK5 activation may be reduced by SATB2.

In contrast to SATB2, SATB1 has been proposed to be a tumor-promoting factor. SATB1 is over-expressed in numerous types of cancer, and its high expression is correlated with metastasis and unfavorable prognosis in patients with malignant melanoma and gastric cancer [28–31]. Additionally, SATB1 expression in breast cancer cells induces dynamic changes in the gene expression profile, and promotes tumor cell proliferation and metastasis [32,33]. A recent study showed that a high level of SATB1 was associated with unfavorable prognosis in colorectal cancer patients, whereas

depletion of SATB1 induced cell-cycle arrest and apoptosis in colorectal cancer cells [34]. Although SATB1 and SATB2 are highly similar at the amino acid level, these two proteins have been reported to have antagonistic functions in embryonic stem cell differentiation [35]. An important area of further research is to determine how the two proteins exert opposing functions in development and tumorigenesis.

In summary, we have shown that SATB2 has a tumor-suppressive function in colorectal cancer cells. Exogenous expression of SATB2 suppressed the aggressive phenotype of colorectal cancer cells. In addition, SATB2 induced the inactivation of ERK5, and constitutive activation of ERK5 conferred a malignant phenotype on SATB2-expressing cells. Further studies to define chromosome architecture and gene profile changes due to SATB2 expression may reveal interesting features of the tumor-suppressive function of SATB2.

## Experimental procedures

### Cells and antibodies

HCT116 and DLD-1 cells were obtained from the American Type Culture Collection (Manassas, VA), and cultured in Dulbecco's modified Eagle's medium (HCT116) or Roswell Park Memorial Institute 1640 (DLD-1), supplemented with 10% fetal bovine serum, penicillin and streptomycin. Cells were authenticated in 2014 by short tandem repeat analysis using the GenePrint® 10 system (Promega, Madison, WI, USA). HEK293T cells for retrovirus production were maintained in Dulbecco's modified Eagle's medium with 10% fetal bovine serum. Antibodies were obtained from the following companies: anti-E-cadherin, anti-N-cadherin and anti-vimentin serums from BD Biosciences (San Jose, CA, USA), anti- $\beta$ -actin serum from Sigma-Aldrich (St Louis, MO, USA), anti-SATB2 serum from Abcam (Cambridge, UK), anti-GFP serum from NeuroMab (Davis, CA, USA), anti-phospho-ERK5 serum (Thr218/Tyr220) from Affinity BioReagents (Golden, CO, USA), anti-ERK5, anti-phospho-ERK1/2, anti-phospho-AKT (Ser473) and anti-AKT serums from Cell Signaling Technology (Danvers, MA, USA), anti-ERK1 serum from Santa Cruz Biotechnology (Santa Cruz, CA, USA) and anti-FLAG serum from Wako (Osaka, Japan).

### Generation of stable cell lines

Full-length SATB2 was PCR-amplified from a cDNA library of HCT116 cells. Full-length SATB2 and the deletion constructs were cloned into the pQCXIP vector (Clontech, Mountain View, CA, USA) with an N-terminal GFP tag, and transfected into HEK293T cells together with the

pVPack-GP and pVPack-Ampho vectors (Promega, Madison, WI, USA) using Lipofectamine 2000 (Invitrogen, Carlsbad, CA, USA). Forty-eight hours after transfection, the supernatants were added to cells along with  $2 \mu\text{g}\cdot\text{mL}^{-1}$  polybrene (Sigma-Aldrich), and infected cells were selected by incubating with  $1 \mu\text{g}\cdot\text{mL}^{-1}$  puromycin for 2 days. Constitutively active and dominant-negative forms of MEK5 were generated by substituting Ser311 and Thr315 with aspartic acid and alanine, respectively, by PCR; the mutants were cloned into the pQCXIP vector with a FLAG tag at the N-terminus. To establish a cell line that constitutively expresses the active form of MEK5 and SATB2, recombinant retrovirus that encoded GFP-SATB2 and active MEK5 were infected into HCT116 cells and selected using 1  $\mu\text{g}/\text{ml}$  of puromycin and 400  $\mu\text{g}/\text{ml}$  of neomycin.

### Colony formation assay

Cells ( $1 \times 10^4$ ) were mixed with 0.36% agar in Dulbecco's modified Eagle's medium supplemented with 10% fetal bovine serum, and overlaid onto a 0.72% agarose layer in six-well plates. After 2 weeks of incubation, the number and size of colonies in five randomly selected fields were counted. Three independent experiments were performed, and values shown are means  $\pm$  SE.

### Invasion assay

To measure cell invasion using Boyden chambers (Corning incorporated, Corning, NY, USA), a filter was pre-coated with Matrigel (Corning incorporated), and  $2 \times 10^5$  cells were seeded onto the upper surface of the chamber. Twenty-four hours after seeding, the cells were fixed with 70% methanol and stained with 0.5% crystal violet. Cells that invaded the lower surface of the filters were counted in five randomly selected fields. Three independent experiments were performed, and values shown are means  $\pm$  SE.

### Wound healing assay

Wound healing assays were performed by scratching confluent monolayers of cells with a pipette tip and incubating the cells at 37 °C with 5% CO<sub>2</sub>. Every 12 h, the distance that the leading edge of the monolayer had traveled was measured in five randomly selected fields. Three independent experiments were performed, and values shown are means  $\pm$  SE.

### Patients and ethics statement

Colorectal cancer samples and normal colorectal tissues were obtained from patients who underwent surgery at Nagoya University Hospital in 2012. For detection of SATB2 expression by quantitative RT-PCR, four normal

colon tissue samples and 21 colorectal cancer tissue samples (stages II–IV) were collected from male and female patients aged 30–60 years. The study was approved by the Institutional Review Board of Nagoya University Hospital, and conformed to the standards set by the Declaration of Helsinki. All participants provided written informed consent to participate in the study.

### Quantitative PCR analysis

RNA was extracted from colorectal cancer samples and cells using an RNeasy Mini Kit (Qiagen, Venlo, The Netherlands), and cDNA was generated using PrimeScript reverse transcriptase (TaKaRa, Tokyo, Japan). PCR was performed using SYBR Premix Ex Taq™ II (TaKaRa), and a TP800 Thermal Cycler Dice™ real time system (TaKaRa) was used for the analysis. The relative mRNA expression levels were normalized to those of glyceraldehyde 3-phosphate dehydrogenase (GAPDH). The sequences of primers used to amplify each gene were 5'-AGGTGGAGGAGTGGGTGTCGCTGT-3' and 5'-CCGGGAAACTGTGGCGTGATGG-3' for GAPDH, and 5'-CTT TGCAAGAGTGGCATTCA-3' and 5'-GTTGTCGGTGTCGAGGTTTT-3' for SATB2.

### Cell proliferation assay

Cells were cultured in 96-well plates, and the number of viable cells at the indicated time points were evaluated using a Cell Counting Kit 8 (Dojindo, Tokyo, Japan).

### Spheroid formation assay

GFP- and GFP-SATB2-expressing HCT116 cells were seeded into Nunclon™ Sphera™ (Thermo scientific, Waltham, MA, USA) six-well plates at a density of  $4 \times 10^4$  cells per well in Dulbecco's modified Eagle's medium containing 10% fetal bovine serum. The cells were incubated at 37 °C with 5% CO<sub>2</sub>, and fresh medium was added after 2–3 days. After 14 days, the number and size of spheres were determined.

### Xenograft tumor assay

Male BALB/c Slc-nu/nu mice (5–6 weeks old) were purchased from Japan SLC (Hamamatsu, Japan). The study was performed in accordance with guidelines issued by the Animal Center at Nagoya University School of Medicine. Animals were housed in covered boxes under controlled temperature and humidity conditions in accordance with the guidelines laid down by the US National Institutes of Health regarding the care and use of animals for experimental procedures. Animals were fed standard mouse chow and water *ad libitum* for an acclimation period of 1 week

prior to initiation of the study protocol. After acclimatization, a total of  $1 \times 10^6$  DLD-1 cells were suspended in 0.1 mL PBS and subcutaneously injected into both sides of the femoral area of the mice. Tumor growth and overall health of the mice were monitored twice per week. The tumor volumes were calculated using the formula length  $\times$  width  $\times$  height/2 (mm<sup>3</sup>). At day 45 post-implantation, the mice were killed in a CO<sub>2</sub> cage, and the tumors were extracted by standard surgery for determination of tumor weight.

### Statistical analysis

All values are mean  $\pm$  SE from three independent assays. All analyses were performed using SIGMAPLOT version 10.0 (Systat Software Inc., San Jose, CA, USA). *P* values were calculated using two-tailed statistical tests. A difference was considered statistically significant when *P* < 0.05.

### Acknowledgements

We would like to thank the members of the Division of Cancer Biology for their helpful discussions. This research was funded by the Naito Foundation and the Ministry of Education, Culture, Sports, Science and Technology of Japan (Nanomedicine Molecular Science, grant number 23107010 to T.S.).

### Author contributions

MM performed most of the experiments. MM and TS designed the experiments. MM, TH and SI analyzed the data. KK, TK, KU and MN prepared cDNAs from colorectal cancer tissues. MM, MT, MH and TS wrote the paper.

### References

- Cunningham D, Atkin W, Lenz HJ, Lynch HT, Minsky B, Nordlinger B & Starling N (2010) Colorectal cancer. *Lancet* **375**, 1030–1047.
- FitzPatrick D, Carr I, McLaren L, Leek J, Wightman P, Williamson K, Gautier P, McGill N, Hayward C, Firth H *et al.* (2003) Identification of SATB2 as the cleft palate gene on 2q32–q33. *Hum Mol Genet* **12**, 2491–2501.
- Britanova O, Akopov S, Lukyanov S, Gruss P & Tarabykin V (2005) Novel transcription factor Satb2 interacts with matrix attachment region DNA elements in a tissue-specific manner and demonstrates cell-type-dependent expression in the developing mouse CNS. *Eur J Neurosci* **21**, 658–668.
- Gyorgy A, Szemes M, De Juan Romero C, Tarabykin V & Agoston D (2008) SATB2 interacts with

- chromatin-remodeling molecules in differentiating cortical neurons. *Eur J Neurosci* **27**, 865–873.
- 5 Dobрева G, Chahrour M, Dautzenberg M, Chirivella L, Kanzler B, Farinas I, Karsenty G & Grosschedl R (2006) SATB2 is a multifunctional determinant of craniofacial patterning and osteoblast differentiation. *Cell* **125**, 971–986.
  - 6 Alcamo E, Chirivella L, Dautzenberg M, Dobрева G, Farinas I, Grosschedl R & McConnell S (2008) Satb2 regulates callosal projection neuron identity in the developing cerebral cortex. *Neuron* **57**, 364–377.
  - 7 Britanova O, de Juan Romero C, Cheung A, Kwan K, Schwark M, Gyorgy A, Vogel T, Akopov S, Mitkovski M, Agoston D *et al.* (2008) Satb2 is a postmitotic determinant for upper-layer neuron specification in the neocortex. *Neuron* **57**, 378–392.
  - 8 Hassan M, Gordon J, Beloti M, Croce C, Van Wijnen A, Stein J, Stein G & Lian J (2010) A network connecting Runx2, SATB2, and the miR-23a~27a–24-2 cluster regulates the osteoblast differentiation program. *Proc Natl Acad Sci USA* **107**, 19879–19884.
  - 9 Beaty T, Hetmanski J, Fallin M, Park J, Sull J, McIntosh I, Liang K, Vanderkolk C, Redett R, Boyadjiev S *et al.* (2006) Analysis of candidate genes on chromosome 2 in oral cleft case-parent trios from three populations. *Hum Genet* **120**, 501–518.
  - 10 Britanova O, Depew M, Schwark M, Thomas B, Miletich I, Sharpe P & Tarabykin V (2006) Satb2 haploinsufficiency phenocopies 2q32-q33 deletions, whereas loss suggests a fundamental role in the coordination of jaw development. *Am J Hum Genet* **79**, 668–678.
  - 11 Leoyklang P, Suphapeetiporn K, Siriwan P, Desudchit T, Chaowanapanja P, Gahl W & Shotelersuk V (2007) Heterozygous nonsense mutation SATB2 associated with cleft palate, osteoporosis, and cognitive defects. *Hum Mutat* **28**, 732–738.
  - 12 Rosenfeld J, Ballif B, Lucas A, Spence E, Powell C, Aylsworth A, Torchia B & Shaffer L (2009) Small deletions of SATB2 cause some of the clinical features of the 2q33.1 microdeletion syndrome. *PLoS One* **4**, 6568.
  - 13 Balasubramanian M, Smith K, Basel-Vanagaite L, Feingold M, Brock P, Gowans G, Vasudevan P, Cresswell L, Taylor E, Harris C *et al.* (2011) Case series: 2q33.1 microdeletion syndrome—further delineation of the phenotype. *J Med Genet* **48**, 290–298.
  - 14 Docker D, Schubach M, Menzel M, Munz M, Spaich C, Biskup S & Bartholdi D (2013) Further delineation of the SATB2 phenotype. *Eur J Hum Genet* **22**, 1034–1039.
  - 15 Dobрева G, Dambacher J & Grosschedl R (2003) SUMO modification of a novel MAR-binding protein, SATB2, modulates immunoglobulin mu gene expression. *Genes Dev* **17**, 3048–3061.
  - 16 Liu T, Xu L, Yang A, Zhong Q, Song M, Li M, Hu L, Chen F, Hu Z, Han P *et al.* (2012) Decreased expression of SATB2: a novel independent prognostic marker of worse outcome in laryngeal carcinoma patients. *PLoS One* **7**, 40704.
  - 17 Wang S, Zhou J, Wang X, Hao J, Chen J, Zhang X, Jin H, Liu L, Zhang Y, Liu J *et al.* (2009) Down-regulated expression of SATB2 is associated with metastasis and poor prognosis in colorectal cancer. *J Pathol* **219**, 114–122.
  - 18 Eberhard J, Gaber A, Wangefjord S, Nodin B, Uhlen M, Lindquist K & Jirstrom K (2012) A cohort study of the prognostic and treatment predictive value of SATB2 expression in colorectal cancer. *Br J Cancer* **106**, 931–938.
  - 19 Yang M, Yu J, Chen N, Wang X, Liu X, Wang S & Ding Y (2013) Elevated microRNA-31 expression regulates colorectal cancer progression by repressing its target gene SATB2. *PLoS One* **8**, 85353.
  - 20 Shah N & Sukumar S (2010) The Hox genes and their roles in oncogenesis. *Nat Rev Cancer* **10**, 361–371.
  - 21 Galande S, Dickinson L, Mian I, Sikorska M & Kohwi-Shigematsu T (2001) SATB1 cleavage by caspase 6 disrupts PDZ domain-mediated dimerization, causing detachment from chromatin early in T-cell apoptosis. *Mol Cell Biol* **21**, 5591–5604.
  - 22 Nithianandarajah-Jones G, Wilm B, Goldring C, Muller J & Cross M (2012) ERK5: structure, regulation and function. *Cell Signal* **24**, 2187–2196.
  - 23 Lochhead P, Gilley R & Cook S (2012) ERK5 and its role in tumour development. *Biochem Soc Trans* **40**, 251–256.
  - 24 Hu B, Ren D, Su D, Lin H, Xian Z, Wan X, Zhang J, Fu X, Jiang L, Diao D *et al.* (2012) Expression of the phosphorylated MEK5 protein is associated with TNM staging of colorectal cancer. *BMC Cancer* **12**, 127.
  - 25 Mehta P, Jenkins B, McCarthy L, Thilak L, Robson C, Neal D & Leung H (2003) MEK5 overexpression is associated with metastatic prostate cancer, and stimulates proliferation, MMP-9 expression and invasion. *Oncogene* **22**, 1381–1389.
  - 26 Barros J & Marshall C (2005) Activation of either ERK1/2 or ERK5 MAP kinase pathways can lead to disruption of the actin cytoskeleton. *J Cell Sci* **118**, 1663–1671.
  - 27 Gong Y, Xu F, Zhang L, Qian Y, Chen J, Huang H & Yu Y (2014) MicroRNA expression signature for Satb2-induced osteogenic differentiation in bone marrow stromal cells. *Mol Cell Biochem* **387**, 227–239.
  - 28 Kohwi-Shigematsu T, Poterlowicz K, Ordinario E, Han H, Botchkarev V & Kohwi Y (2013) Genome organizing function of SATB1 in tumor progression. *Semin Cancer Biol* **23**, 72–79.
  - 29 Cheng C, Lu X, Wang G, Zheng L, Shu X, Zhu S, Liu K, Wu K & Tong Q (2010) Expression of SATB1 and

- heparanase in gastric cancer and its relationship to clinicopathologic features. *APMIS* **118**, 855–863.
- 30 Lu X, Cheng C, Zhu S, Yang Y, Zheng L, Wang G, Shu X, Wu K, Liu K & Tong Q (2010) SATB1 is an independent prognostic marker for gastric cancer in a Chinese population. *Oncol Rep* **24**, 981–987.
- 31 Chen H, Takahara M, Oba J, Xie L, Chiba T, Takeuchi S, Tu Y, Nakahara T, Uchi H, Moroi Y *et al.* (2011) Clinicopathologic and prognostic significance of SATB1 in cutaneous malignant melanoma. *J Dermatol Sci* **64**, 39–44.
- 32 Yanagisawa J, Ando J, Nakayama J, Kohwi Y & Kohwi-Shigematsu T (1996) A matrix attachment region (MAR)-binding activity due to a p114 kilodalton protein is found only in human breast carcinomas and not in normal and benign breast disease tissues. *Cancer Res* **56**, 457–462.
- 33 Han H, Russo J, Kohwi Y & Kohwi-Shigematsu T (2008) SATB1 reprogrammes gene expression to promote breast tumour growth and metastasis. *Nature* **452**, 187–193.
- 34 Fromberg A, Rabe M & Aigner A (2014) Multiple effects of the special AT-rich binding protein 1 (SATB1) in colon carcinoma. *Int J Cancer* **135**, 2537–2546.
- 35 Savarese F, Davila A, Nechanitzky R, De La Rosa-Velazquez I, Pereira C, Engelke R, Takahashi K, Jenuwein T, Kohwi-Shigematsu T, Fisher A *et al.* (2009) Satb1 and Satb2 regulate embryonic stem cell differentiation and Nanog expression. *Genes Dev* **23**, 2625–2638.